


 Cite this: *RSC Adv.*, 2023, **13**, 11728

# A thermochromic poplar-based tetradecyl ester/methyl composite encapsulated with PEG400–SiO<sub>2</sub> (PS-R-PTC) for improving thermal energy storage

Yanqiang Tong, Weihua Zou, \* Delin Sun and Zhangheng Wang

Thermochromic wood is an important research direction for wood modification in recent years, and a red poplar-based thermochromic composite (R-PTC) had been prepared in our previous study by compositing a mixture of phase change reagents (tetradecyl ester: C<sub>28</sub>H<sub>56</sub>O<sub>2</sub> and methyl red: C<sub>15</sub>H<sub>15</sub>N<sub>3</sub>O<sub>2</sub>) and full poplar wood. In order to improve the heating storage ability of R-PTC and encapsulating phase change reagents to prevent leakage, a new R-PTC composite (PS-R-PTC) was prepared by encapsulated R-PTC with polyethylene glycol 400 (PEG400)–SiO<sub>2</sub> in this work. Compared to the original R-PTC samples, the cell walls of PS-R-PTC were not significantly changed by the SiO<sub>2</sub> film and we also found that PS-R-PTC with PEG400 (90%)–silica solutions (10%) mixture had better heat storage performance and PS-R-PTC (90%) has better enthalpy change value (R-PTC: 43.01 J g<sup>-1</sup>; PS-R-PTC (90%): 71.82 J g<sup>-1</sup>). The PS-R-PTC can show the function of thermal energy storage, which is used in wooden buildings and can be a feasible insulating material for reducing thermal energy losses and hence reducing energy usage. In PS-R-PTC, SiO<sub>2</sub> combines with the –OH of the R-PTC and the –OH of PEG400 (HO(CH<sub>2</sub>CH<sub>2</sub>O)<sub>n</sub>H), and these –OH lose hydrogen ions too.

Received 13th March 2023

Accepted 2nd April 2023

DOI: 10.1039/d3ra01640d

rsc.li/rsc-advances

## 1. Introduction

The issue of thermal energy is an important energy problem facing human society today.<sup>1</sup> As a key component of various domestic and industrial processes and power generation systems, thermal energy storage ensures system reliability, power transmission, and profitability.<sup>2</sup> It is a well-established fact that buildings are the world's largest consumers of energy. In the EU, buildings use almost 40% of the electricity consumed, which directly leads to significant carbon emissions.<sup>3</sup> In the United States, heating, ventilation and air conditioning (HVAC) operations account for approximately 40% to 60% of overall energy use in institutional and conventional buildings. In China, about 65% of rural households need heating in winter. Due to cold weather, a lot of energy is wasted by maintaining the temperature of the building.<sup>4</sup> Therefore, solving the problem of energy consumption in human society has become the focus of current scientific research.

Fossil fuels are now the main source of building heating storage. However, the consumption of non-renewable resources and environmental pollution makes people pursue new energy solutions.<sup>5</sup> As compared to fossil fuels, phase change materials (PCMs) have been widely used due to their large heat storage capacity and lesser volume change during the phase change process.<sup>6</sup> PCMs have been widely used in heat storage to

improve energy management in heat pumps,<sup>7,8</sup> solar engineering<sup>9,10</sup> and air conditioning facilities,<sup>11–13</sup> for instance. Therefore, research into the energy and heat storage of phase change materials and the enhancement of their heat storage effect is currently a hot topic of research.

In our previous study, a red poplar-based thermochromic composite (R-PTC) was prepared by filling a mixture of phase change reagents (tetradecyl ester: C<sub>28</sub>H<sub>56</sub>O<sub>2</sub> and methyl red: C<sub>15</sub>H<sub>15</sub>N<sub>3</sub>O<sub>2</sub>) into poplar. This type of R-PTC can undergo a colour change from light-red to dark-red at about 38 °C to 46 °C and can revert to light-red at below 38 °C after about 14 h.<sup>14</sup> Liquid leakage is one of the inherent disadvantages of phase-change materials.<sup>15–17</sup> The research in this paper is designed to further improve the thermal storage performance of R-PTC and to reduce the leakage of phase-change reagents from R-PTC.

Polyethylene glycol (PEG) is an organic phase change material for polyethers, and it is a long-chain polymer consisting of –CH<sub>2</sub>CH<sub>2</sub>O– with hydroxyl groups at both ends and exhibits good hydrophilicity.<sup>18–20</sup> In this work, the mixture of liquid reagent polyethylene glycol (PEG400) and neutral silica sol was added to the prepared R-PTC for improving its phase changeability. In this experiment, different mass ratios of PEG400 and silica solutions were dipped into R-PTC, and three PS-R-PTC samples were obtained by vacuum impregnation. The samples were tested by differential scanning calorimetry (DSC) and it was found that the PS-R-PTC had the highest enthalpy of phase change. The PS-R-PTC was analysed by scanning electron

Central South University of Forestry and Technology, Shaoshan South Road 498, Changsha, 410004, China. E-mail: weibick@sina.cn



microscopy (SEM) for internal structure and energy dispersive spectrometry (EDS) for elemental content. After the above experiments, it was found that the phase change reagent was well encapsulated in the poplar substrate by the action of PEG400 and  $\text{SiO}_2$ . The Fourier transform infrared spectroscopy (FTIR) spectra before and after warming (10–60 °C) were collected for monitoring functional groups and structural changes.

## 2. Experimental

### 2.1 Materials and chemicals

Longitudinal-cutting polar veneer (thickness: 5.0 mm) slices with dimensions of  $40 \times 40 \times 10$  mm were purchased from Mudan Wood Co., Ltd. (Suqian, China). R-TD ( $\text{C}_{28}\text{H}_{56}\text{O}_2$  and  $\text{C}_{15}\text{H}_{15}\text{N}_3\text{O}_2$ ) and the NaOCl solution were obtained from Kermel Chemical Reagent Co., Ltd., polyethylene glycol 400 (PEG400,  $\text{HO}(\text{CH}_2\text{CH}_2\text{O})_n\text{H}$ , molecular weight: 400) was obtained from Kermel Chemical Reagent Co., Ltd., (Tianjin, China), and neutral silica sol (solid content of  $\text{SiO}_2$ : 30%) was purchased from Aladdin Biochemical Technology (Shanghai, China).

### 2.2 Preparation of PS-R-PTC

The poplar veneer was first dried and immersed in NaOCl solution and steamed with deionized water. R-TD ( $\text{C}_{28}\text{H}_{56}\text{O}_2$  and  $\text{C}_{15}\text{H}_{15}\text{N}_3\text{O}_2$ ) was prepared and a thicker, poplar-based, thermochromic composite (R-PTC, thickness: 5.0 mm) was prepared by the infiltration of red thermochromic dyes (R-TD) into the pre-treated poplar veneer (thickness: 5.0 mm) and compacting the resulting poplar-based composite. Finally, the R-PTC was compacted and coated with polypropylene wax.

PEG400 and  $\text{SiO}_2$  with different mass ratios were obtained by melting and blending, followed by the ultrasonic method. Table 1 shows the quality ratio of the PEG400 and  $\text{SiO}_2$  (P-S) mixture. PEG400 and  $\text{SiO}_2$  were divided into three different mass fraction ratios: 100%, 90%, and 80%. Number: PS-80, PS-90, and PS-100. The three reagents were stirred for about 0.5 h at about 45 to 50 °C and left for an hour to mix the two solutions well. Three kinds of PEG400– $\text{SiO}_2$  were obtained (Fig. 1).

The R-PTC slices were dried at 90 °C. The samples were dried. The PS-R-PTC were prepared by vacuum filling the PEG400– $\text{SiO}_2$  into R-PTC specimens at 80 °C and evacuated under 1 kPa. In the process, the vacuum oven pump was switched off to allow the air to enter, thereby forcing the PEG400– $\text{SiO}_2$  reagent to seep into the R-PTC, and this process was repeated three times. Thereafter, the PS-R-PTC was placed on a paper and heated to 50 °C the phase-transition

Table 1 The chemical formula and method of PS-R-PTC

Method	Chemicals (g, ml)
Treatment of sample 1	PEG400 (10 g), neutral silica sol (0 g)
Treatment of sample 2	PEG400 (9 g), neutral silica sol (1 g)
Treatment of sample 3	PEG400 (8 g), neutral silica sol (2 g)

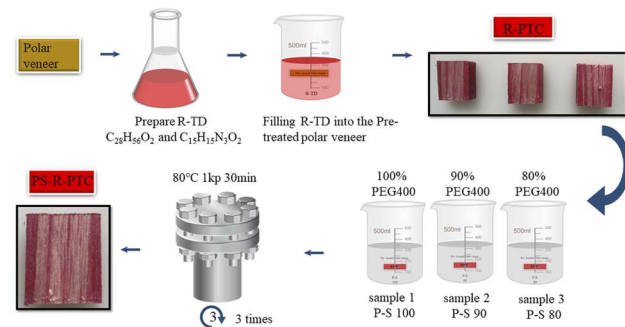


Fig. 1 Preparation of the PS-R-PTC material.

temperature of PEG400– $\text{SiO}_2$  to remove the redundant PEG400– $\text{SiO}_2$  and until no leakage of the molten PEG400– $\text{SiO}_2$  was observed.

### 2.3 Performance testing of PS-R-PTC

The three samples were first tested by the infrared thermometer to compare the cooling rate after warming up to 80 °C. The differential scanning calorimetry (DSC) was performed to examine the phase change enthalpy, maximum phase change temperature, and phase change temperature of the three samples. After data analysis and comparison, the PS-R-PTC with the best thermal storage capacity was analyzed by scanning electron microscopy (SEM) to observe its internal structure. The PS-R-PTC was then subjected to Fourier transform infrared (FTIR) to analyze the changes in functional groups and chemical bonds.

## 3. Results and discussion

### 3.1 Infrared thermometer test of PS-R-PTC

The samples were heated to 80 °C in the oven, and then placed in a room temperature environment at 5 °C. The temperature of the samples was measured by an infrared thermometer every 3 minutes to compare the cooling rate. Fig. 2 shows the cooling rates of these three samples, and the PS-R-PTC of PS-90 is the

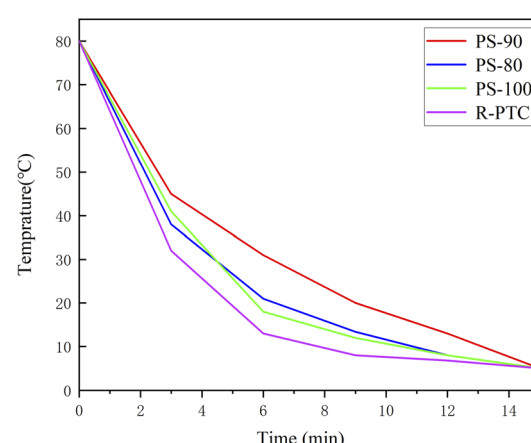


Fig. 2 Cooling rates of the PS-R-PTC materials and R-PTC.



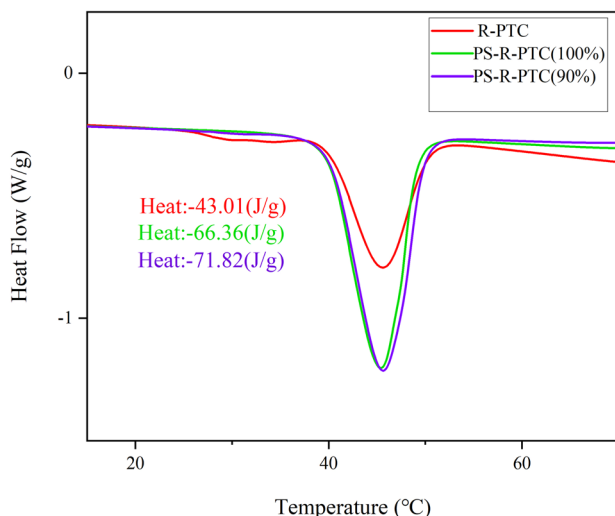


Fig. 3 DSC patterns of PS-R-PTC and R-PTC.

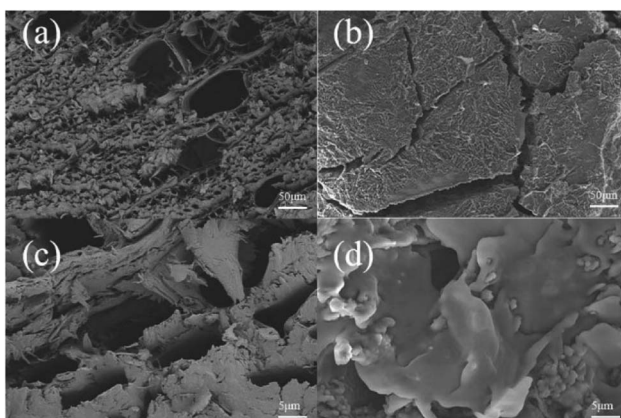


Fig. 4 (a and c) Micrograph of R-PTC. (b and d) Micrograph of PS-R-PTC.

best in the heating storage of the samples. This experiment was carried out 50 times and the cooling curves of these specimens were found to be essentially similar, thus demonstrating the stability of PS-R-PTC in thermal energy storage.

### 3.2 DSC test of PS-R-PTC

DSC was used to measure the phase change properties of PS-R-PTC. 100%, 90%, and 80% mass ratio PEG400 treated with neutral silica sol reagent were tested in the experiments. Fig. 3 shows the DSC curves of the composite phase change energy storage material. As can be seen from the graphs (Fig. 3), the curves of R-PTC and PS-R-PTCs give the enthalpy of the phase change, the maximum melting temperature, and the phase change temperature. Fig. 3 shows that the PS-R-PTCs had a greater enthalpy change and better thermal storage than R-PTC. Compared to R-PTC, PS-R-PTC (90%) has a better enthalpy change value (R-PTC:  $43.01\text{ J g}^{-1}$ ; PS-R-PTC (90%):  $71.82\text{ J g}^{-1}$ ).

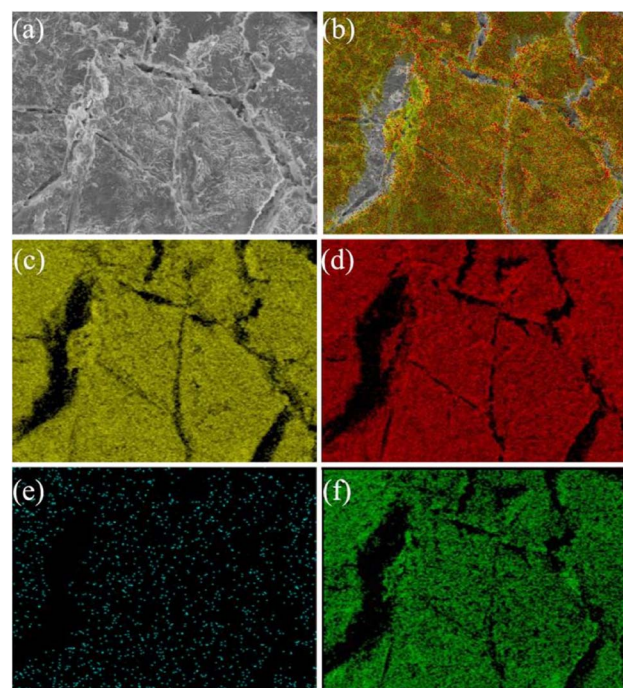
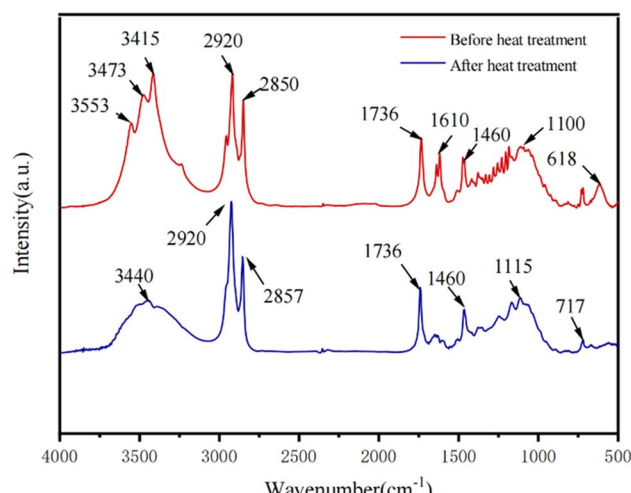


Fig. 5 The EDS testing of PS-R-PTC: (a and b) mapping detect area image and all elements mapping, (c-f) element mapping images of C, O, N and Si on the surface and inside the pores.

Fig. 6 FTIR spectra: before heat treatment, and after heat treatment ( $60\text{ }^\circ\text{C}$ ) PS-90-R-PTC specimens.

Analysis shows that as the mass fraction of PEG400 in the impregnating reagent of the R-PTC samples increases, the phase change enthalpy of the samples increases and then decreases. This is because the terminal hydroxyl groups of PEG400 and the C-O-C in the chains will bond with the cellulose, hemicellulose, and aliphatic components of the wood through hydrogen bonding and mutual adsorption. This indicates that poplar wood in the mixture not only acts as a diluting agent but also affects the crystallinity of PEG.<sup>21</sup> When the



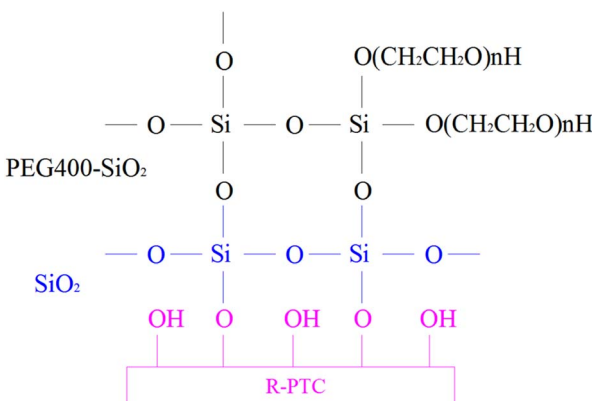


Fig. 7 The combined mechanism of PS-R-PTC.

content of PEG400 is too high, too much PEG400 will leak into the wood pores, limiting the freedom of the PEG chains in the phase change temperature range and resulting in a lower enthalpy of phase change. Due to the complexity of the wood itself, it is difficult to achieve a certain content of polyethylene glycol and its uniform distribution in the wood, which are important factors in the enthalpy of phase change and phase transition temperature.<sup>22,23</sup> Therefore, a certain proportion of neutral silica sol reagent was added to reduce the leakage of PEG400 and improve its phase change capacity. The phase change enthalpy was increased compared to that of the pristine R-PTC, which has an enhanced phase change heat storage capacity. From the data in the table, it was concluded that 90% by mass of the PEG400 reagent was impregnated as impregnating reagent in the PS-R-PTC material to bring out the better phase change capability of the PS-R-PTC material. We chose PS-90 as the impregnating reagent for PS-R-PTC for the next experiments.

### 3.3 Microscopic features of PS-R-PTC

The microscopic features of phase change materials (PCMs) were examined by SEM.<sup>24,25</sup> The microscopic features of PS-R-PTC were examined by a Sigma 300 scanning electron microscope (SEM, ZEISS, Germany) Fig. 4(a) and (c). The SEM images of the R-PTC samples are shown in Fig. 4(a) and (c), which show microscopic images of the original R-PTC, and Fig. 4(b) and (d) show R-PTC impregnated with a mixture of PEG400 and neutral silica sol with a mass fraction of PEG400 of 90%. The electron microscopic analysis of the R-PTC (Fig. 4(a) and (c)) was compared with that of the PS-R-PTC (Fig. 4(b) and (d)). It can be observed that the wood apertures on the surface of R-PTC are filled with PEG400-SiO<sub>2</sub>. In comparison with the rough and irregular surface of R-PTC, the surface of PEG400-SiO<sub>2</sub> (90%) PS-R-PTC was smooth and even. The porous spaces of PS-R-PTC were filled with PEG400 and had significantly fewer visible pores at different magnifications, indicating the successful absorption of PEG400 into PS-R-PTC. Where it was found that compared to the original R-PTC sample, the mixture of SiO<sub>2</sub> solids and PEG400 can be observed filling the R-PTC wood cell lumen, with no significant thickening of the cell wall due to the

SiO<sub>2</sub> support, as shown in the micrographs of radial-cut and longitudinal-cut samples.

### 3.4 EDS test of PS-R-PTC

Energy-dispersive X-ray spectroscopy (EDS) data of the PEG400-SiO<sub>2</sub> sample confirmed that all elements in the catalyst were: C, Si, N, and O, and all the elements were uniformly distributed on the catalyst particles. The C, N, O, and Si contents were 72.23%, 0.01%, 15.70%, and 12.06%, respectively. Fig. 5(a) shows the selected area of EDS mapping, and the element composition and distribution of the synthesized catalyst material are shown in Fig. 5(b-f). According to the results of EDS, some elements, C, O and Si, should come from PEG400 (HO(CH<sub>2</sub>CH<sub>2</sub>O)<sub>n</sub>H)-SiO<sub>2</sub>, the heating storage material that was successfully filled into PS-R-PTC.

### 3.5 FTIR spectra comparison of PS-R-PTC before and after heat treatment

FTIR spectra analysis is as Fig. 6 shown. The prepared PS-R-PTC (PS-90) was heated and treated to compare the infrared spectra before heating (red line) with those after heating to 60 °C (blue line). By comparing curves a, and b in Fig. 6, it was found that PS-R-PTC showed a stretching vibrational absorption peak corresponding to C-H and a bending vibrational absorption peak at 2920 cm<sup>-1</sup>, 1460 cm<sup>-1</sup>, and 1330 cm<sup>-1</sup>, respectively, and the observation curve revealed that the stretching vibrational absorption peak of -OH broadened at 3415 cm<sup>-1</sup> and shifted to the lower frequency band, indicating that the H-atom on -OH formed a hydrogen bond, and since the raw material of R-PTC, poplar wood, contains cellulose, hemicellulose and lignin extracts contained small amounts of fatty acids, the stretching vibration absorption peak of -OH at 3440 cm<sup>-1</sup> and the carbonyl peak at 1736 cm<sup>-1</sup> appeared.<sup>26</sup> The absorption peak at 1100 cm<sup>-1</sup> is the result of the superposition of the C-O-C stretching vibration absorption peak of PEG400 and the anti-symmetric stretching vibration absorption peak of the C-O-C bond in poplar wood.<sup>27</sup> Thus, in this experiment, the impregnation of R-PTC with a mixture of PEG400 and neutral silica sol reagents did not show any significant chemical reaction between them before the heating test, and heating to 60 degrees celsius is favourable for the full use of the phase change energy storage of polyethylene glycol.

### 3.6 Combination mechanism of PS-R-PTC

According to the formation mechanism of -O-Si-CH<sub>3</sub>,<sup>28,29</sup> PS-R-PTC was formed by filling R-PTC with PEG400 and SiO<sub>2</sub> to form PEG400-SiO<sub>2</sub> (Fig. 7), which was tested to improve the phase change capability and thermal storage performance of the original R-PTC. The combined mechanism of PS-R-PTC is shown in Fig. 7. According to the combination form of -O-Si-O- and -OH from wood and the -OH lost hydrogen ion,<sup>30</sup> so SiO<sub>2</sub> combined between the -OH of the R-PTC and the -OH of PEG400 (HO(CH<sub>2</sub>CH<sub>2</sub>O)<sub>n</sub>H), and these -OH lost hydrogen ions too.



## 4. Conclusions

In this study, the phase change reagent PEG400 and neutral silica sol reagent were added to the R-PTC reagent by pressure impregnation. It was found that PS-R-PTC with 90% mass of PEG400 had better heating storage performance and higher enthalpy of the phase change ( $71.82 \text{ J g}^{-1}$ ), so we selected PS-90 as the impregnating reagent. We performed SEM electron microscopic analysis of this PS-R-PTC and found that PEG400 was able to fill the wood cell lumen, and did not change significantly the cell wall due to the  $\text{SiO}_2$  film. FTIR spectra analysis of this PS-R-PTC showed that PEG400 did not form a chemical change in the wood. Our PS-R-PTC can be used for temperature indication and thermal energy storage in building facades for insulation of wooden floors, and as energy-saving materials for indoor environments.

## Conflicts of interest

There are no conflicts to declare.

## Acknowledgements

This work was financially supported by the Scientific Research Project of the Education Department of Hunan Province, China (No. 22A0185); the Hunan Provincial Natural Science Foundation of China (No. S2023JJMSXM0333).

## Notes and references

- 1 X. Chen, P. Cheng, Z. Tang, X. Xu, H. Gao and G. Wang, *Adv. Sci.*, 2021, **8**(9), 2001274.
- 2 W. Aftab, A. Usman, J. Shi, K. Yuan, M. Qin and R. Zou, *Energy Environ. Sci.*, 2021, **14**(8), 4268–4291.
- 3 X. Cao, X. Dai and J. Liu, *Energy Build.*, 2016, **128**, 198–213.
- 4 X. Duan, Y. Jiang, B. Wang, X. Zhao, G. Shen, S. Cao, N. Huang, Y. Qian, Y. Chen and L. Wang, *Appl. Energy*, 2014, **136**, 692–703.
- 5 K. Kaygusuz, *Renewable Sustainable Energy Rev.*, 2012, **16**, 1116–1126.
- 6 P. B. Salunkhe and P. S. Shembekar, *Renewable Sustainable Energy Rev.*, 2012, **16**, 5603–5616.
- 7 A. A. Pardonas, M. J. Alonso, R. Diz, K. H. Kvalsvik and J. F. Seara, *Energy Build.*, 2017, **140**, 28–41.
- 8 S. Rashidi, H. Shamsabadi, J. A. Esfahani and S. Harmand, *J. Therm. Anal. Calorim.*, 2019, **140**, 1655–1713.
- 9 M. H. Abokersh, M. Omnia, O. El-Baz, M. El-Morsi and O. Sharaf, *Int. J. Energy Res.*, 2017, **42**, 329–357.
- 10 M. Mofijur, T. M. I. Mahlia, A. S. Silitonga, H. C. Ong, M. Silakhori, M. H. Hasan, N. Putra and S. M. A. Rahman, *Energies*, 2019, **12**, 31–67.
- 11 I. Sarbu and C. Sebarchievici, *Solar Heating and Cooling Systems: Fundamentals, Experiments and Applications*, Elsevier, Oxford, UK, 2016.
- 12 M. Sokolov and Y. Keizman, *Sol. Energy*, 1991, **47**(5), 339–346.
- 13 W. Wu, X. Huang and K. Li, *Appl. Energy*, 2017, 474–480.
- 14 W. Zou, Z. Li, Z. Wang, D. Sun and P. Zhang, *Sci. Rep.*, 2021, **11**, 16865.
- 15 D. G. Atinafu, W. Dong and U. Berardi, *Chem. Eng. J.*, 2020, **394**, 124806.
- 16 H. Zhang, Z. Liu, J. Mai, *et al.*, *Chem. Eng. J.*, 2021, **411**, 128482.
- 17 C. Y. Wang, L. L. Feng, W. Li, J. Zheng, W. H. Tian and X. G. Li, *Sol. Energy Mater. Sol. Cells*, 2012, **105**, 21–26.
- 18 S. Zhao, J. Li and S. Song, *J. Energy Storage*, 2022, **51**, 104416.
- 19 C. Xu, W. Wang, H. Zhang, *et al.*, *Sol. Energy Mater. Sol. Cells*, 2023, **250**, 112093.
- 20 M. A. Marcos, D. Cabaleiro, M. J. G. Guimarey, *et al.*, *Nanomaterials*, 2017, **8**(1), 16.
- 21 S. Grandi, A. Magistris, P. Mustarelli, E. Mustarelli, C. Tomasi and L. Tomasi, *J. Non-Cryst. Solids*, 2006, **352**(3), 273–280.
- 22 Z. Liu, H. Wei, B. Tang, S. Xu and Z. Shufen, *Sol. Energy Mater. Sol. Cells*, 2018, **174**, 538–544.
- 23 S. Zhang, H. Zhao, B. Zhao and L. Du, *J. Polym. Sci.*, 2004, **3**, 388–393.
- 24 C. Xie, *et al.*, *Sci. Silvae Sin.*, 2012, **48**, 120–126.
- 25 L. Bin, L. Xiang, L. Renpu, T. Weiping, Y. Zhuohong and Y. Teng, *Sol. Energy Mater. Sol. Cells*, 2019, **200**, 110037.
- 26 X. Jiaqi, Y. Tiantian, X. Xing, X. Guo and G. Jinzhen, *Composites, Part A*, 2020, **139**, 106098.
- 27 Q. Meijie, G. Chuigen, L. Liping and Z. Xiucheng, *J. Therm. Anal. Calorim.*, 2017, **130**, 781–790.
- 28 D. Briggs and G. Beamson, *Chem*, 1992, **64**, 1729.
- 29 Y. Jie, Q. Guoqiang, L. Yang, B. Ruiying, L. Zhengying, Y. Wei, X. Banghu and Y. Mingbo, *Carbon*, 2016, **100**, 693–702.
- 30 Y. Meng, Y. Zhao, Y. Zhang, *et al.*, *Chem. Eng. J.*, 2020, **390**, 124618.

